Journal of Agricultural Science; Vol. 14, No. 4; 2022
ISSN 1916-9752 E-ISSN 1916-9760
Published by Canadian Center of Science and Education

# Advanced Damage Assessment Method for Bacterial Leaf Blight Disease in Rice by Integrating Remote Sensing Data for Agricultural Insurance

Chiharu Hongo[1], Yusuke Takahashi[2], Gunardi Sigit[3], Budi Utoyo[3] & Eisaku Tamura[1]

[1] Center for Environmental Remote Sensing, Chiba University, Chiba, Japan

[2] JA ZENNOH CHIBA, Chiba, Japan

[3] Regional Office of Food Crops Service West Java Province, West Java, Indonesia

Correspondence: Chiharu Hongo, Center for Environmental Remote Sensing, Chiba University, 1-33 Yayoi-cho, Inage-ku, Chiba-shi, Chiba 263-8522, Japan. E-mail: hongo@faculty.chiba-u.jp

Received: January 3, 2022 Accepted: February 20, 2022 Online Published: March 15, 2022

doi:10.5539/jas.v14n4p1 URL: https://doi.org/10.5539/jas.v14n4p1

*The research is financed by Japan Science and Technology Agency (JST) and JICA. Grant Number: JPMJSA1604.*

**Abstract**

This study aimed to develop a new method for assessing damage to rice plants by pests and diseases using remote sensing data to enable greater efficiency and accuracy for payment of indemnity in the agricultural insurance system of Indonesia, formally operationalized in 2016. The relationships between bacterial leaf blight (BLB) damage ratio in rice crops evaluated by pest observers using the current visual inspection method and the reflectance of each observation band of RapidEye and Sentinel 2, normalized difference vegetation index (NDVI), green NDVI (GNDVI), and red edge multiplied by the green band index (RGI) were studied. The results showed a positive relationship between BLB damage intensity and reflectance of visible wavelength bands, and a particularly strong positive correlation between the red band and BLB damage intensity. The BLB damage intensity can be evaluated based on pixels and paddy parcels. Time series analysis was conducted using Sentinel-2 data acquired during different plant growth periods such as heading, flowering, ripening, maturity, and harvesting. The results showed a strong correlation between the BLB damage intensity and reflectance of the red edge band at the rice heading and flowering stages; the correlation of BLB damage intensity with the reflectance of the visible range became stronger as the rice plant approached the harvesting stage. This study clearly demonstrated that BLB symptoms can be successfully detected and evaluated approximately one or one and a half months before the harvesting period using remote sensing data. We propose that the BLB damage intensity, currently assessed by pest observers through visual inspection methods, can be calculated from satellite data, suggesting that the satellite sensor could play a role similar to the human eye.

**Keywords:** food security, remote sensing, pest and diseases, RapidEye, Sentinel-2, Indonesia

## 1. Introduction

Global climate change and natural disasters are anticipated to exert a substantial impact on food production worldwide, and adaptation measures to mitigate this impact have attracted considerable attention. In their fifth assessment report, the Intergovernmental Panel on Climate Change (IPCC) has predicted a high probability of negative impact of climate change on food crops (IPCC, 2014). A particularly severe influence is indicated on the production of food crops from the viewpoint of food security, and on the life of the poor owing to the loss of food crops because of temperature increase and rainfall, food shortage, and increase in food prices. In addition, low-latitude areas are reported to be at a higher risk of decreased food security. The food security vulnerability and impact of climate change can reduce the speed of economic growth and induce socio-economic disadvantages. To resolve this situation, the concept of agricultural insurance was introduced and has now gradually disseminated internationally. Agricultural insurance is an important social infrastructure to secure stability, which is defined as one of the four pillars of food security by the Food and Agriculture Organization

(FAO, 2006). Agricultural insurance, through its role as a socio-economic process, is now widely considered to be a promising adaptation measure against crop damages caused by climate change. In the IPCC Special Report on Food Security (IPCC, 2019), agricultural insurance is described as an example of an effective measure to promote adaptation. Thus, agricultural insurance aims to reduce damages caused by climate change, support farmers to continue agricultural production, and contribute in realizing the food security of a country.

ASEAN countries are facing several different problems, such as an increase in population, decrease in cultivable area, and influence of climate change. Food security is one of the key concerns for these countries and Indonesia is no exception. Indonesia has the fifth largest population (approximately 267 million) among the countries in the world (FAO, 2014), with a rate of increase of approximately 1% per year, which is expected to continue (FAOSAT, 2018a). Rice is a staple food in Indonesia, with the third largest production in the world (FAOSAT, 2018b). A few years ago, the country managed to reach a level of self-sufficiency; however, climate change caused an increase in crop damage owing to floods, droughts, pests, and diseases, resulting in reduced rice yields. In 1996, 1997, and 2006, rice was imported from other countries. This experience triggered a debate among the people in the government and agriculture-related fields on the necessity of introducing and disseminating an agricultural insurance system in Indonesia to ensure its food security. Acknowledging this need, the Government of Indonesia, through the Ministry of Agriculture, initiated several pilot projects of the agriculture insurance program in 2012 to minimize the risk of production failure, particularly in rice farming. After trials through the pilot projects, the agricultural insurance system was formally operationalized in 2016.

A key aspect in agricultural insurance is damage assessment, which should be precise and quick inexpensive to the maximum extent possible. As an approach to satisfy such requirements, the introduction of innovative technologies, including remote sensing technology, to the insurance procedure is expected to be highly prioritized. The current damage assessment method for rice in West Java in Indonesia involves visual inspection by a damage assessor called a pest observer. The assessment involves selection of three paddy fields as sampling plots on a diagonal line in an area of approximately 10-20 ha and, 10 clumps are visually observed in each plot and evaluated against six damage grades. One pest observer is assigned per district for the evaluation of approximately 5,000–10,000 ha. Therefore, there is a significant time lapse between assessment and the payment of indemnity, which in certain cases occurs when it becomes difficult for farmers to start transplanting rice for the next cultivation season. In this situation, the provincial governments have keen interest in developing new methods that can facilitate damage assessment with less time, costs and labor. To comply with these needs, we started a project called Science and Technology Research Partnership for Sustainable Development (SATREPS) supported by the Japanese and Indonesian governments in 2017. This project aims to develop and implement an integrated damage assessment method that utilizes remote sensing technology for greater effectiveness. The main damage-causing agents of our project targets are pests and diseases, drought and floods. Among different plant pests and diseases, the project focuses on the bacterial leaf blight (BLB) disease of rice. The assessment of BLB using remote sensing has been addressed in a few previous studies, such as the monitoring and evaluation of BLB occurrence using remote sensing data in Kannur, India (Das et al., 2015), and the development of a regression model to evaluate BLB damage through optical checking of specific disease features on rice plants in Taiwan (Chwen-Ming, 2010). However, research on BLB using remote sensing data is still very rare; moreover, no such prior research has been conducted in Indonesia.

Our study area was located in West Java that witnesses serious BLB damage every year. The study aimed to check whether this damage can be assessed using remote sensing data and also if a new evaluation formula could be developed by integrating a method that utilizes satellite data with the current method. This report provides a summary of our study results.

## 2. Methodology

### *2.1 Study Area*

The study area was situated at lat. 6°50′S. and long. 107°16′E in the Cihea irrigation district, northeast of Cianjur, West Java, Indonesia. The climate in this region is temperate throughout the year because of the tropical climate near the equator. It has both a dry season (April to August) and a wet season (November to March of the following year). Rice plantings are performed two to three times a year. This study was conducted during the first planting of the dry season.

In Cihea, rice is produced using large-scale irrigation systems. Rice diseases, particularly BLB, occur throughout the year. The average paddy parcel size is approximately 500 $m^2$, with non-uniform parcel shape. Each parcel has a different planting time, which results in a mixture of paddies at different growth stages.

*2.2 BLB*

BLB is a disease caused by the bacterium *Xanthomonas oryzae* and is highly prevalent in Asian countries, including Japan, India, Indonesia, and Sri Lanka. In Southwest Asia, including Indonesia, BLB occurs frequently and regularly causes substantial damage, depending on the year.

BLB gains entry into the rice plants through the water pore apertures of the rice leaves or wounds on the plant surface caused by wind or rain (Krishnan et al., 2009). Research using bacteriophages has clearly revealed that the infection route of the bacterium involves passing into the irrigation water and spreading to other areas.

The symptoms of the disease are as follows: first, the edge of the rice leaf becomes yellow; a boundary part of the leaf between the yellowed edge and healthy central part of the leaf becomes wavy; subsequently, the color of the yellow part changes to yellowish-white, and finally to white. The picture in Figure 1, captured at our study site, shows the symptoms of the disease on rice leaves. The effect of BLB on rice yield is as follows: when rice is infected at an early growth stage, a lesion is formed on the leaf, thereby reducing the leaf area for absorption of nutrients and efficient photosynthesis; this leads to a decrease in the number of tillers, which finally leads to a reduction in rice yield. Infection during the ripening period directly reduces the yield. However, when the rice is infected just before the harvesting period, yield is less affected, even after the appearance of a large lesion on the leaf.

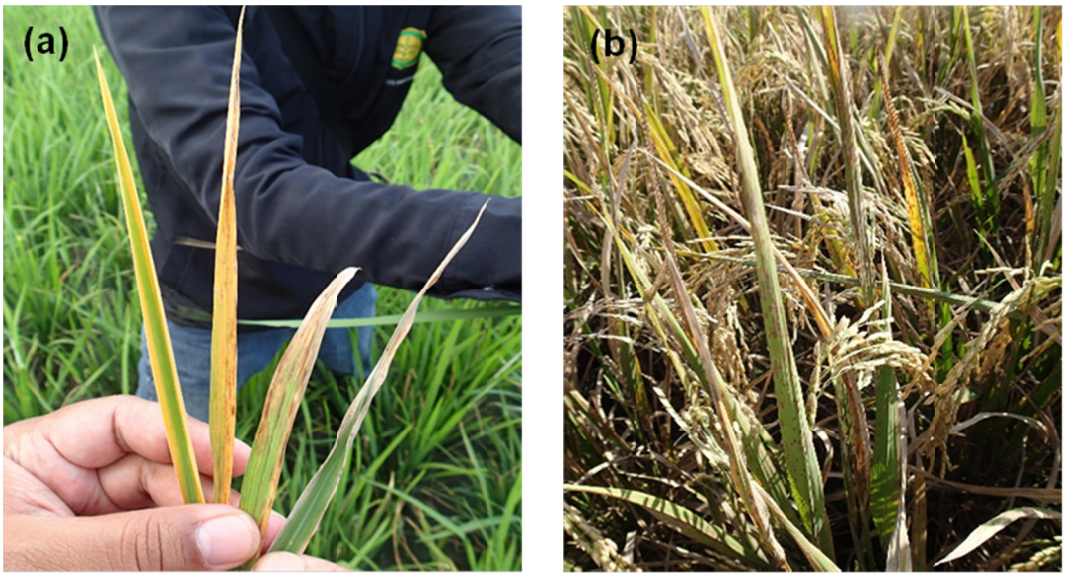


Figure 1. Symptoms of bacterial leaf blight (BLB) on (a) rice leaves and (b) rice crop

*2.3 Data for Analysis*

2.3.1 On-Site Field Investigation Data

Field investigations were conducted from July 30 to August 2, 2017, on approximately 22 paddy fields ready for harvesting. The investigated items included the BLB damage degree, GPS data of the investigated location, transplanting date, and rice variety. The four main rice varieties cultivated in the study area are IR64, Ciherang, Sintanur, and Mekongga, and their cultivation periods are 116-120 days, 116-125 days, 115-125 days, and 115-126 days, respectively. Although the cultivation period differs depending on the variety, it is roughly 120 days on average.

The BLB infection in the selected study area during the investigation period differed significantly from that reported in 2016, and was spread throughout the study area, with almost no paddy plot spared from the infection. Among the plots, a few had severe damage (over 70%). The following points were considered while selecting a paddy plot for investigation: it should be at the pre-harvesting stage; it should cover a wide area within the study area; it should include all the different damage levels from light to heavy.

The BLB damage degree was evaluated by pest observers. The evaluation procedures were in accordance with the guidelines formally issued by the Indonesian government. In the current agricultural insurance system,

indemnity is calculated based on the evaluation results. The evaluation of BLB damage and calculation of the damage intensity were conducted using the following procedure. First, three paddy plots were selected for sampling on a diagonal line in the assigned investigation area (Figure 2); 10 clumps in each selected plot were visually inspected by the pest observer with regard to the number of tillers, color and appearance of leaf, and condition of rice ears. Then, the BLB damage degree was determined according to six grades: 0 = 0%, 1 = 1-20%, 3 = 21-40%, 5 = 41-60%, 7 = 61-80%, 9 = 81-100%. Finally, the determined damage value of each clump was input into the following equation to calculate the BLB damage intensity.

$$\text{BLB damage intensity } (\%) = (n_1 + n_2 + \ldots + n_{10})/(9 \times 10) \quad (1)$$

Where, n: BLB damage degree of each clump using the six grades.

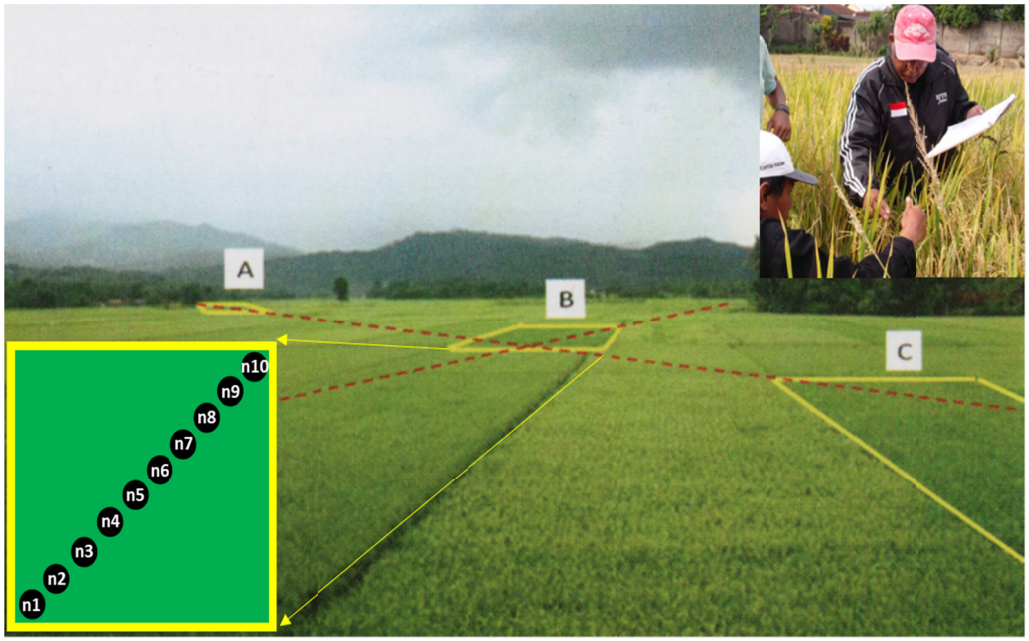


Figure 2. Investigation area

2.3.2 Satellite Data

RapidEye data obtained on July 17, 2017, and Sentinel-2 data obtained on June 14, July 4, and July 19, 2017, were used to analyze and determine the extent of BLB infection.

Because the images for analysis were acquired at different times with different sensors, the digital value of the spectral band has to be converted to ground reflectance. Therefore, the data for analysis were obtained using the following reflectance conversion equation (PLANET.COM, 2016).

$$\text{RAD}(i) = \text{DN}(i) \times \text{radiometric ScaleFactor}(i) \quad (2)$$

$$\text{REF}(i) = \text{RAD}(i) \times \frac{\pi \cdot \text{SunDist}^2}{\text{EAI}(i) \cdot \cos(\text{SolarZenith})} \quad (3)$$

Where, RAD: Radiance value ($W/m^2/sr/\mu m$); i: Number of the spectral band; DN: Digital value of the spectral band; radiometric ScaleFactor: radiometric ScaleFactor(i) = 0.01; REF: Reflectance value (%); SunDist: Earth-Sun distance on the day of acquisition in astronomical units (AU); EAI: Exo-atmospheric irradiance ($w/m^2/\mu m$); For RapidEye, the EAI values for the five bands are as follows: Blue: 1997.8 $W/m^2\mu m$; Green: 1863.5 $W/m^2\mu m$, Red: 1560.4 $W/m^2\mu m$, RE: 1395.0 $W/m^2\mu m$, NIR: 1124.4 $W/m^2\mu m$; SolarZenith: Solar zenith angle in degrees.

The Earth-Sun distance on the day of acquisition in astronomical units can be calculated using the following equation, while the Julian date ($J$) is confirmed from the date of satellite image acquisition.

$$\text{SunDist} = 1.0000 + 0.01676 \times \cos\{0.977 \times (J - 186)\} \quad (4)$$

The SolarZenith angle can be calculated with the following equation using the solar elevation angle at the time of capturing the satellite image, which is recorded in the metadata file.

$$\text{SolarZenith} = 90\text{degree} - \text{SolarElevation} \quad (5)$$

In this study, Sentinel-2 images were used after level 1C processing. This product is created using DEM to project the images on a cartographic coordinate system. The radiometric scale factor by pixel is input as the top of atmosphere (TOA) reflectance value in the parameter and then converted to radiance. Therefore, for analysis, the radiance has to be reconverted to the TOA reflectance value using the following numerical expression (Ferran et al., 2016).

$$\text{TOA} = \frac{\text{DN value of Each band}}{10000} \quad (6)$$

In addition, to compare the reflectance of data acquired at different times with different sensors, their bit numbers should be the same. RapidEye has 32-bit whereas Sentinel-2 has 12-bit data. Therefore, in this study, the Sentinel-2 data were converted to 32 bits for equivalence with those of RapidEye, using the images after reflectance conversion.

*2.4 Research Procedure*

Reflectances at the blue, green, red, near infrared (NIR), and red edge bands were extracted from the RapidEye and Sentinel-2 images after geometric correction, reflectance conversion, and bit number conversion. The images were captured at the locations where the pest observers had evaluated the BLB damage degree. Following the government guidelines for BLB infection evaluation, approximately 10 clumps per paddy plot were visually inspected, and the damage intensity was calculated. The intensity is considered to represent the entire investigated plot. Therefore, reflectance data were extracted from the pixels of the satellite images of the sampling plots, and the average of the reflectance data was used as the reflectance per paddy plot. In addition, using the reflectance data, the red edge multiplied by the green band index (RGI), normalized difference vegetation index (NDVI), and green normalized difference vegetation index (GNDVI) were calculated.

Then, the relationships among reflectances at each band of RapidEye data, the three indexes, and BLB damage intensity were analyzed. The time of onset of symptoms related to BLB infection was checked using a chronological analysis of three images from Sentinel-2 data acquired at different times. Finally, a numerical formula to estimate the damage intensity was created by employing multiple regression analysis using the least squares method, with the BLB damage intensity as an objective variable and each band and the indexes as explanatory variables. Moreover, the coefficient of determination was calculated to confirm the accuracy of the regression analysis, and the estimation formula was verified using 10-hold cross validation.

## 3. Results and Discussion

The analysis of the relationship between the reflectance at each band of RapidEye data, the three indexes, and BLB infection intensity are shown in Figure 3. The RapidEye data were obtained on July 17, 2017, which was approximately two weeks before the on-site investigation during the harvesting season. Scatter diagrams between the BLB damage intensity and the blue, green, red, and red edge bands as well as RGI were created, which confirmed a clear tendency that the higher the BLB damage intensity is, the larger the reflectance value becomes at each band and index. As observed in all the diagrams, the determination and correlation coefficients exceed 0.5 and 0.7, respectively, which indicates a strong linear relation. Particularly, the determination and correlation coefficients are higher in the diagrams with blue, green, and red bands, which are in the visible range. The highest values of the determination and correlation coefficients are 0.653 and 0.808, respectively, both of which correspond to the red band. As for NDVI and GNDVI, which are frequently used for vegetation research, the results confirmed that the higher the BLB damage intensity is, the smaller the reflectance value becomes at each band and index. The determination and correlation coefficients of NDVI were 0.526 and -0.725, respectively, indicating a strong linear relationship. The determination and correlation coefficients for GNDVI were 0.425 and -0.652, respectively, indicating a moderate linear relationship. The NDVI and BLB damage intensity have a strong relationship with each other, and their strength is approximately the same as that of the red edge band and RGI. However, the relationship between reflectance at near infrared and BLB damage intensity is not clear, and both the determination and correlation coefficients have low values.

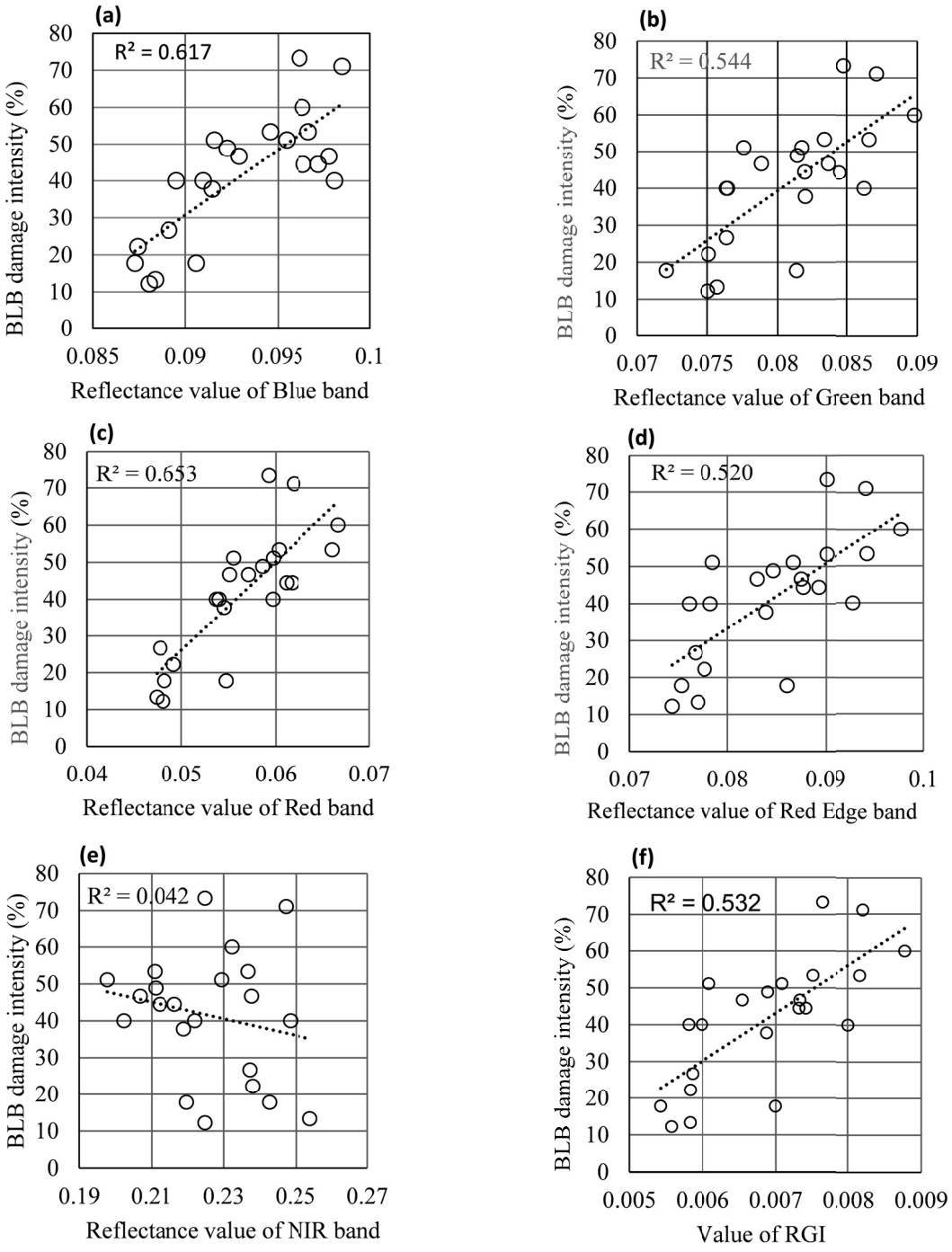
(a)
R² = 0.617
BLB damage intensity (%)
Reflectance value of Blue band
(b)
R² = 0.544
BLB damage intensity (%)
Reflectance value of Green band
(c)
R² = 0.653
BLB damage intensity (%)
Reflectance value of Red band
(d)
R² = 0.520
BLB damage intensity (%)
Reflectance value of Red Edge band
(e)
R² = 0.042
BLB damage intensity (%)
Reflectance value of NIR band
(f)
R² = 0.532
BLB damage intensity (%)
Value of RGI

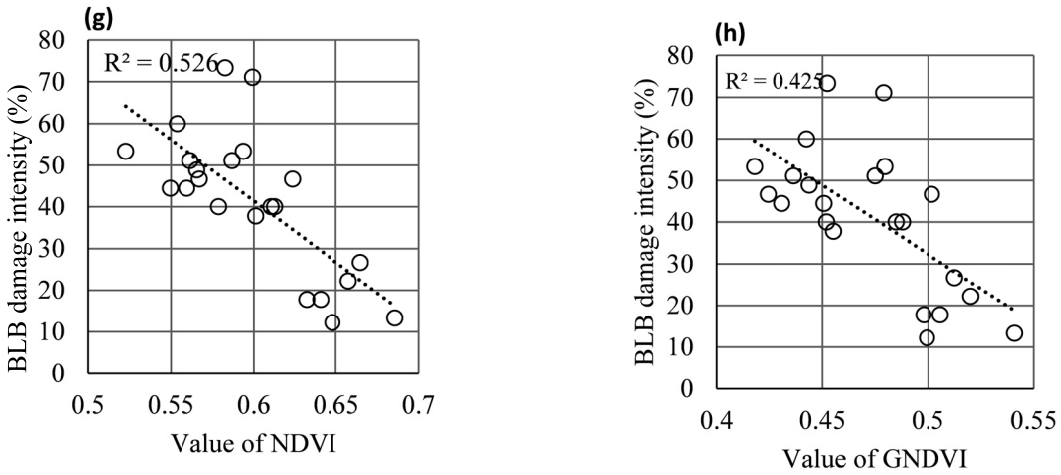


Figure 3. Relationships between bacterial leaf blight (BLB) damage intensity and RapidEye image: (a) Blue band, (b) Green band, (c) Red band, (d) near infrared (NIR) band, (e) Red edge band, (f) red edge multiplied by the green band index (RGI) (g) normalized difference vegetation index (NDVI), and (h) green NDVI (GNDVI)

The BLB symptoms show the following progression: first, the edge of the leaf near the leaf tip becomes yellowish green; the leaf edge then gradually yellows; as the disease progresses, the yellow part changes to yellowish-white and finally becomes white. In case of serious disease, the leaf is dehydrated and curls up. It acquires a straw-like color, and after losing all color, finally withers (Encyclopedia Britannica, 2020). Paddy with this level of serious damage appears whitish. Examples of paddy with different levels of BLB damage in our study are shown in Figure 4.

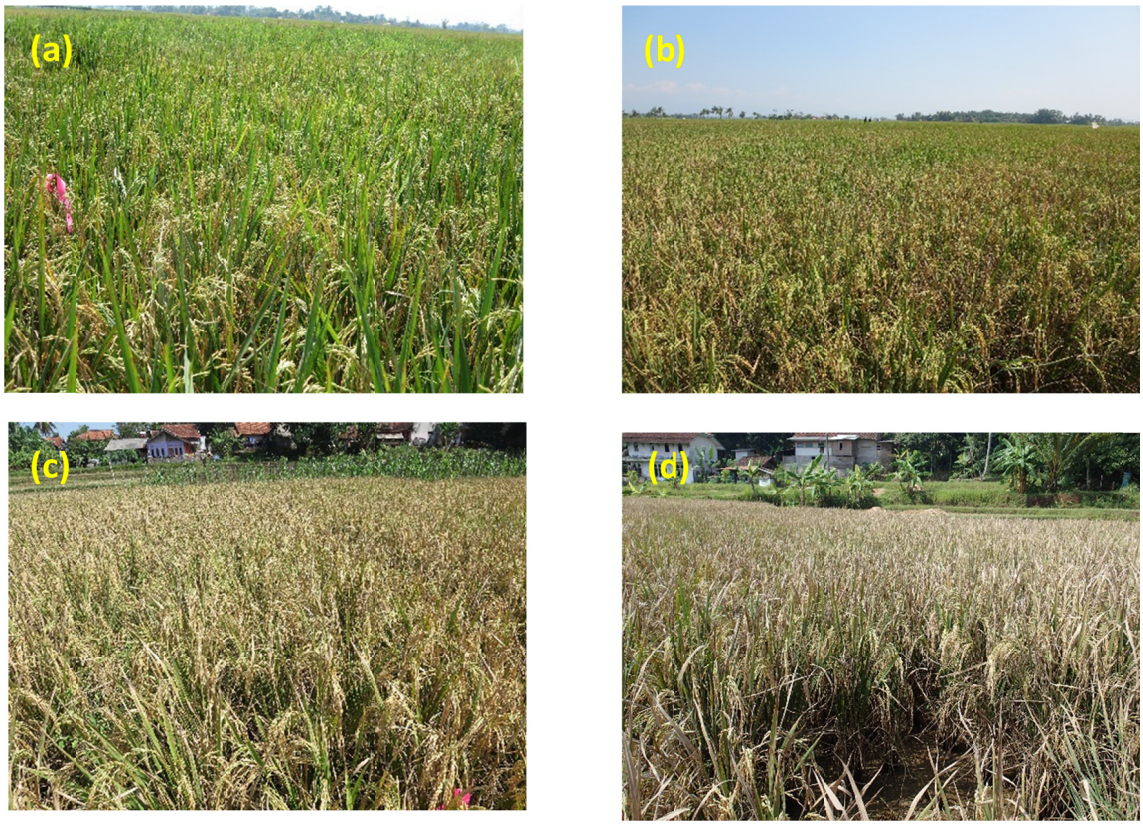


Figure 4. Paddy pictures with different intensities of bacterial leaf blight (BLB);
(a) 17%, (b) 46%, (c) 71%, (d) 74%

The figure shows that the paddy sample with 73% damage intensity appears more decolored and exhibits greater straw-like color than that with 17% damage intensity. This remarkable symptom is considered to support a high positive correlation of BLB damage intensity with blue, green, and red bands, which are closely related to the reflectance of leaf colors. The red edge is a wavelength zone between 680 nm and 750 nm in the reflection spectrum of the plant, and the reflectance changes drastically in the zone. The red edge changes slightly according to the growing conditions of the plants, indicating the level of vigor and chlorophyll content in them (Clevers & Lammert, 2012; Cleversa & Gitelsonb, 2013; Zhou et al., 2017). When rice is infected with BLB, chlorophyll in the leaves is decomposed and leads to loss of vitality in the rice plant, resulting in changes in the green color of the leaves. This can explain the positive correlation of the red edge band and RGI with the degree of BLB infection. It is well known that the reflectance of the NIR band is related to the biomass volume and production amount of crops (Taifeng et al., 2020; Julian et al., 2020). When rice plants are infected at an early growing stage, the number of tillers reduces compared with those of healthy rice plants. A lower number of tillers indicates a decreased biomass volume. In our study, although a slight negative correlation was observed between the reflectance of the NIR band and BLB damage intensity, a substantial correlation could not be observed. The reason for this observation may be the occurrence of the BLB infection after the tillering stage, and the rice plants may have already gained a measurable amount of biomass at the time of our investigation in the harvesting season.

The results confirmed a positive relationship between satellite images captured approximately two weeks before harvesting and the BLB damage intensity at harvesting time. Therefore, to check the time BLB symptoms started to appear in the investigated paddy plots and the time lapse before a relation could be confirmed between the BLB damage intensity and satellite data, time-series analysis was performed using three Sentinel-2 images captured at three different periods.

The time-series change in the relation between the BLB damage intensity and the reflectance of each band and index is shown in a total of 36 images (Figures 5 to 10), using satellite images acquired on June 14, July 4, and July 19. Sentinel-2 has three red edge bands: 690-720 nm (Band 5), 725-755 nm (Band 6), and 763-803 nm (Band 7); they are depicted in the figures as Red edge1_Band5, Red edge2_Band6, and Red edge3_Band7. RGI, which is the mathematical product of the red and green bands, is represented here as GRI1_Band5, RGI2_Band6, and RGI3_Band7. Small, round colored symbols in the figures depict different levels of the damage intensity, that is, green-, yellow green-, yellow-, orange-, and red-colored symbols represent 0-30%; 30-40%; 40-50%; 50-60%, and 60-80% damage, respectively. The damage intensity data were calculated from the data obtained in the harvesting season between July 30 and August 2, 2017. The relation between the acquisition date of satellite data and rice growing stage is as follows: satellite data captured on June 14 represents the heading and flowering stage, that on July 4 the ripening and maturity stage, and that on July 19 the harvesting stage.

Analysis of the data obtained on June 14 showed no relation between the BLB damage intensity and any one of the blue, green, or red bands, red edge1_Band5, GRI1_Band5, or NDVI. All the damage intensity values were almost the same. In contrast, despite the low determination coefficient, a relation was observed at 1-5% significant level between the BLB damage intensity and each of Red edge2_Band6, Red edge3_Band7, NIR, RGI2_Band6, RGI3_Band7, and GNDVI (Table 1).

The data on July 4, approximately 20 days later, exhibited a relation opposite to that on June 14. Specifically, a relationship was observed at a 1% significance level between the BLB damage intensity and each of the blue, green, red, Red edge1_Band5, and GRI1_Band5 bands, and the coefficient of determination was over 0.5 (Table 1). In case of the blue band, the determination and correlation coefficients were 0.4748 and 0.689, respectively, which indicates a moderate linear relation; in the other four cases, the coefficients were a little below 0.6 and approximately 0.7, respectively, indicating a strong linear relation. With regard to Red edge2_Band6, Red edge3_Band7, NIR, and RGI3_Band7 bands, no significant relation was observed.

Approximately two weeks later on July 19, the relationship between BLB damage intensity and each of blue and green bands was weaker when compared with the data on July 4; however, the relationship between BLB damage intensity and each of red, Red edge1_Band5, and GRI1_Band5 bands strengthened, with correlation and determination coefficients greater than 0.8 and 0.6, respectively, at 1 % significance level (Table 1).

As for NDVI and GNDVI, which are commonly used to check vegetation conditions, June 14 data indicate a gradually increasing tendency in their values after a slight increase in the BLB damage intensity; however, a few other results indicated a random relationship between these indexes and BLB damage intensity. On the other hand, July 4 data show a different tendency when compared with those on June 14. The two indexes decrease with increasing BLB damage intensity, and in the case of approximately 50% BLB damage intensity, they show insignificant change. In paddy fields with low BLB damage intensities, the two indexes were relatively higher.

Thus, these findings demonstrated that the higher the BLB damage intensity is, the lower the NDVI and GNDVI indexes become.

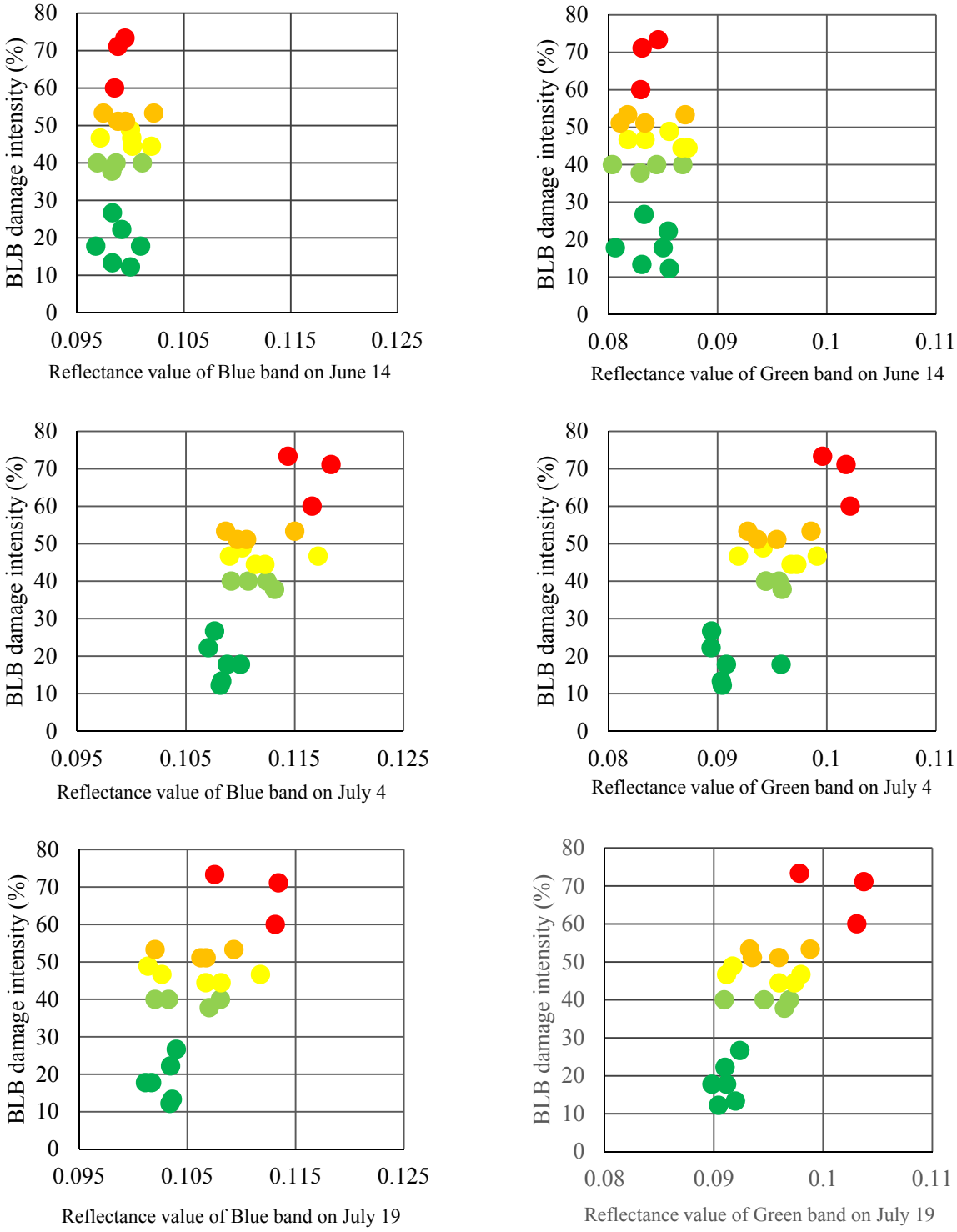


Figure 5. Relation between bacterial leaf blight (BLB) damage intensity and the blue and green bands of Sentinel-2 data on three different dates

*Note*. ● 0-30% damage, ● 30-40% damage, ● 40-50% damage, ● 50-60% damage, ●60-80% damage.

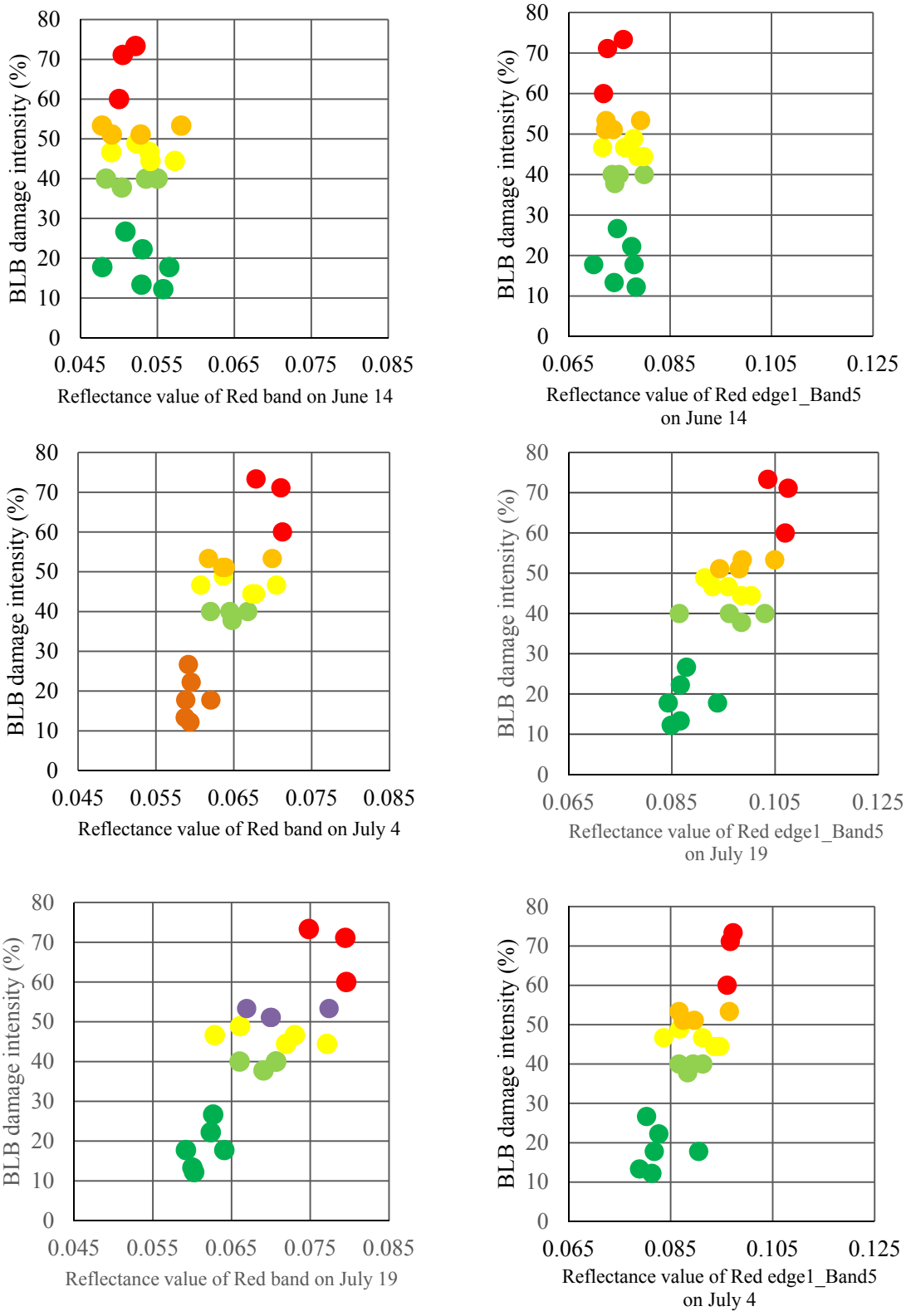


Figure 6. Relations between bacterial leaf blight (BLB) damage intensity and red and Red edge1_band5 bands of Sentinel-2 data on three different dates

*Note*. ● 0-30% damage, ● 30-40% damage, ● 40-50% damage, ● 50-60% damage, ●60-80% damage.

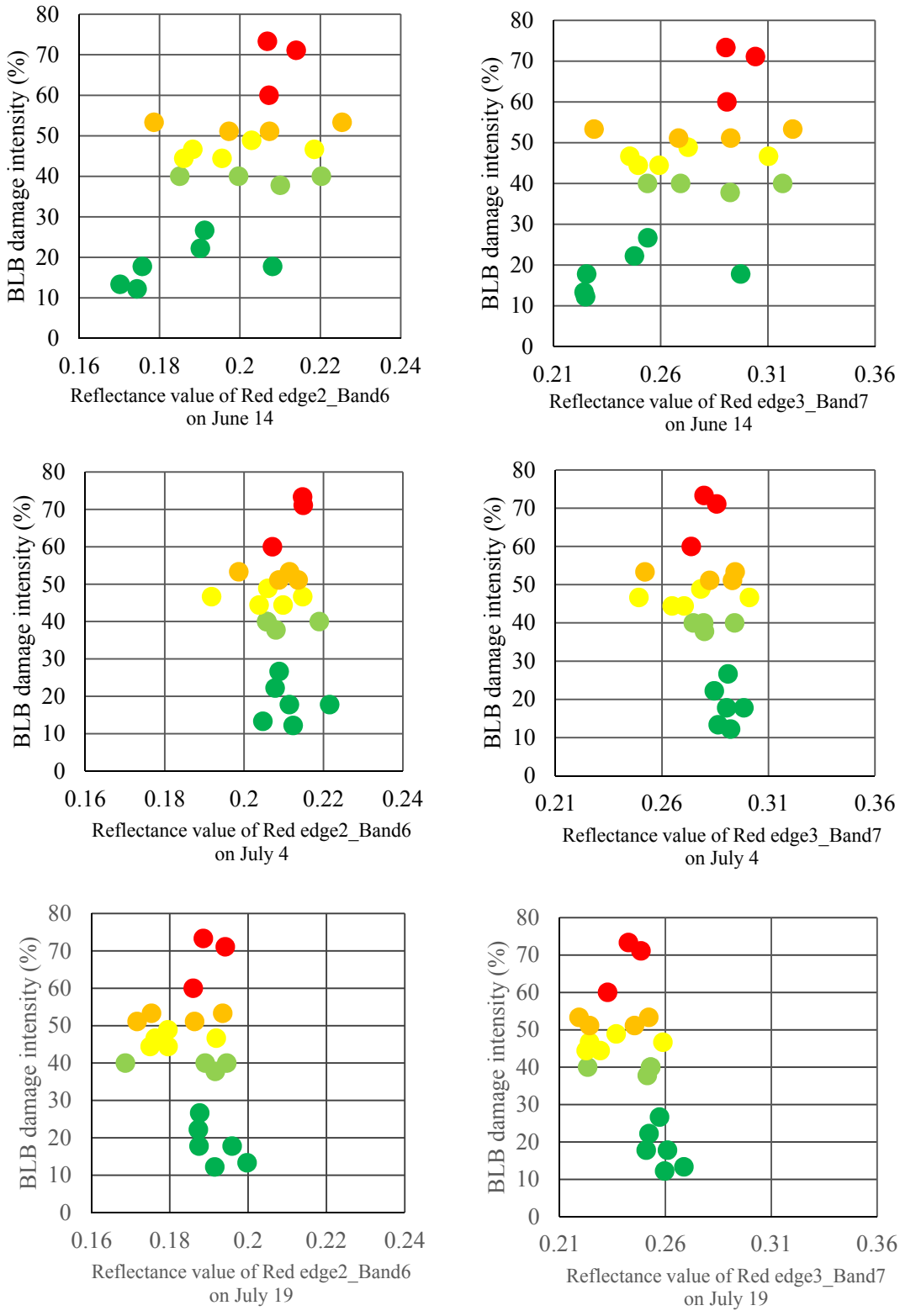


Figure 7. Relations between bacterial leaf blight (BLB) damage intensity and Red edge2_band6 and Red edge3_band7 bands of Sentinel-2 data on three different dates

*Note*. ● 0-30% damage, ● 30-40% damage, ● 40-50% damage, ● 50-60% damage, ●60-80% damage.

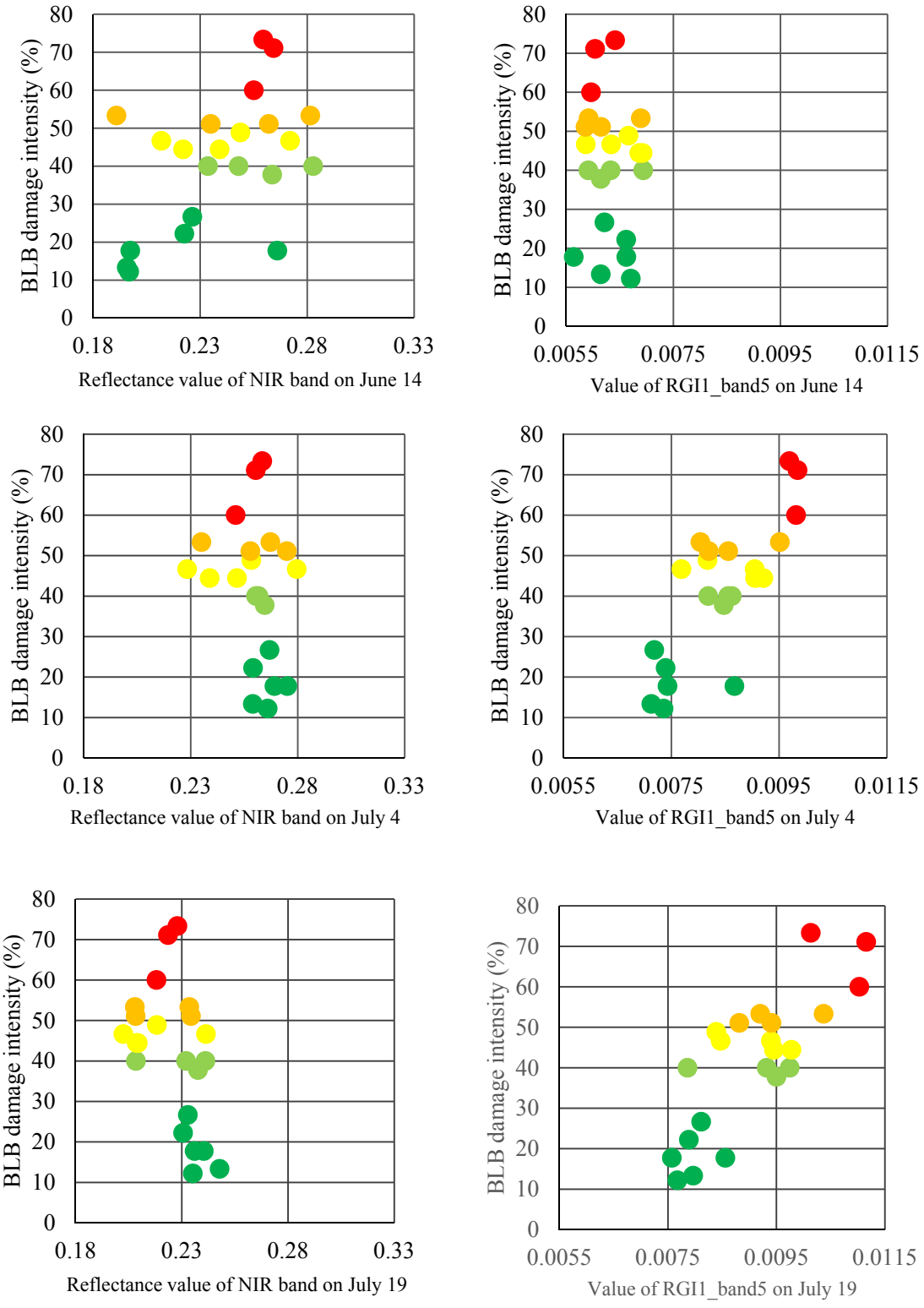


Figure 8. Relations between bacterial leaf blight (BLB) damage intensity and near infrared (NIR) and RGI1_band5 bands on three different dates

*Note*. ● 0-30% damage, ● 30-40% damage, ● 40-50% damage, ● 50-60% damage, ●60-80% damage.

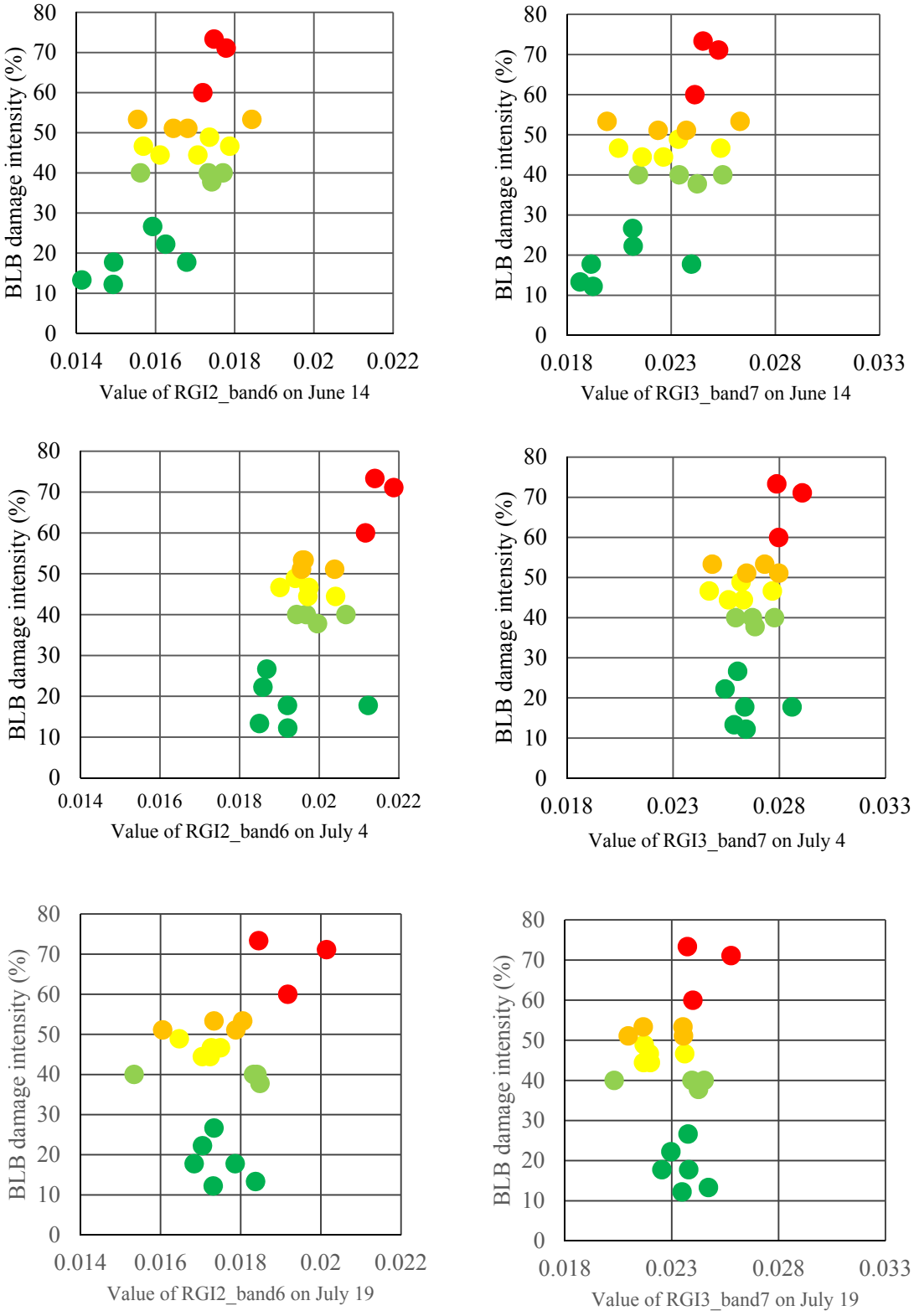


Figure 9. Relations between bacterial leaf blight (BLB) damage intensity and RGI2_band6 and RGI3_band7 bands on three different dates

*Note*. ● 0-30% damage, ● 30-40% damage, ● 40-50% damage, ● 50-60% damage, ●60-80% damage.

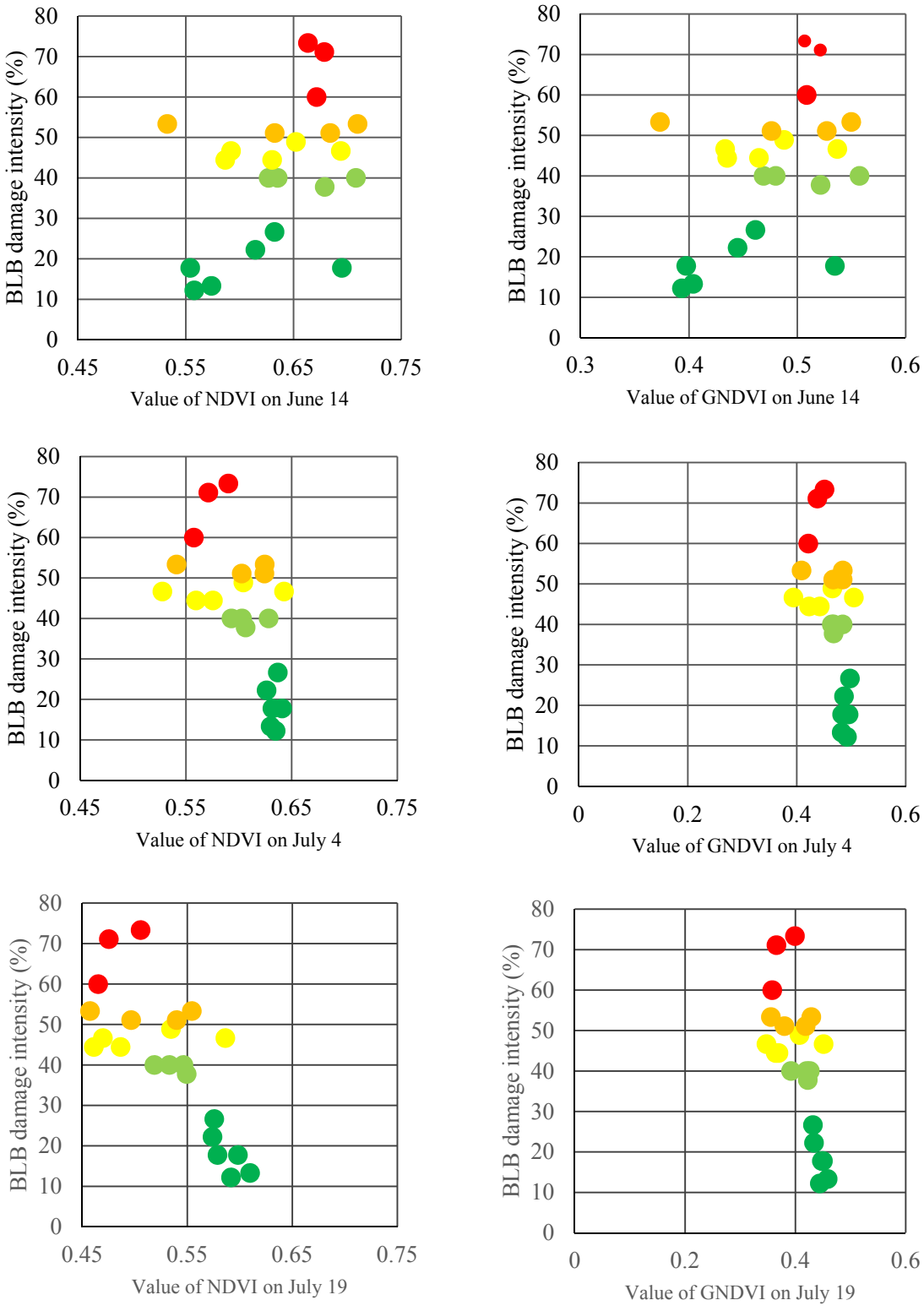


Figure 10. Relations between bacterial leaf blight (BLB) damage intensity and normalized difference vegetation index (NDVI) and green NDVI (GNDVI) on three different dates

*Note*. ● 0-30% damage, ● 30-40% damage, ● 40-50% damage, ● 50-60% damage, ●60-80% damage.

Table 1. Determination and correlation coefficients between bacterial leaf blight (BLB) damage intensity, each band of Sentinel-2 data, and indices on three different dates in 2017

| | June 14 | | July 4 | | July 19 | |
|---|---|---|---|---|---|---|
| | $R^2$ | r | $R^2$ | r | $R^2$ | r |
| Blue band | 0.0072 | 0.086 | 0.4748 | 0.689** | 0.3723 | 0.610** |
| Green band | 0.0005 | -0.022 | 0.5737 | 0.757** | 0.5388 | 0.734** |
| Red band | 0.0328 | -0.181 | 0.5722 | 0.756** | 0.6621 | 0.814** |
| Red edge (B5) | 0.0191 | -0.138 | 0.5874 | 0.766** | 0.6453 | 0.803** |
| Red edge (B6) | 0.3001 | 0.548** | 0.0032 | -0.056 | 0.0759 | -0.275 |
| Red edge (B7) | 0.2810 | 0.530* | 0.1035 | -0.322 | 0.2681 | -0.518* |
| NIR band | 0.2329 | 0.483* | 0.0602 | -0.245 | 0.2132 | -0.462* |
| RGI (B5) | 0.0090 | -0.095 | 0.5998 | 0.774** | 0.6401 | 0.800** |
| RGI (B6) | 0.4059 | 0.637** | 0.3626 | 0.602** | 0.0993 | 0.315 |
| RGI (B7) | 0.3669 | 0.606** | 0.1094 | 0.331 | 0.00007 | -0.008 |
| NDVI | 0.1646 | 0.406 | 0.3354 | -0.579** | 0.5543 | -0.745** |
| GNDVI | 0.1907 | 0.437* | 0.2940 | -0.542** | 0.4537 | -0.674** |

*Note*. **: 1% of significant level; *: 5% of significant level.

Based on the above results, the following can be summarized: According to the reflectance data of the visible region and Red edge1_band5 captured on June 14, it is difficult to judge the presence or absence of BLB infection. However, using the reflectance data of the visible region and Red edge1_band5 acquired on July 4 and July 19, it is possible to judge the presence of BLB infection on rice and also to evaluate the BLB damage intensity. In addition, by focusing on the red edge band and the index using the red edge, it is possible to check the change in the values in healthy rice plants in fields with greater than 50% damage intensity, even if no change in reflectance is observed in the visible range.

In 2017, it was assumed that the rice plants in the study area were infected by BLB at the heading and flowering stages on June 14, and at the time of harvesting, the plants showed 60–80% BLB damage intensity. As the rice plants were infected after the tillering stage, the plants had almost no damage to the stems, leaves, etc. when compared with the same parts of healthy plants. Therefore, it is suggested that although a relationship with reflectance in the NIR band of RapidEye data could not be observed, it is closely related to the biomass amount. In addition, the results indicate that, depending on the wavelength to be used, the BLB infection levels can be successfully detected and assessed if investigation is performed around one or one and a half months before the harvesting season.

After reviewing all the above results regarding BLB damage intensity and satellite data, it was our consideration that the damage evaluation result obtained by the pest observer through the visual inspection method could be expanded to a wider area using satellite data. Therefore, the BLB damage intensity was first estimated from satellite data using multiple regression analysis. RapidEye images acquired on July 17, 2017 were used for the analysis using a stepwise procedure. Consequently, the following equation was created to estimate the BLB damage intensity using reflectance of red band at 1% significance level.

$$\text{BLB damage intensity (\%)} = 4490.031 \times \text{Red band} - 376.032 \quad (7)$$

The BLB damage intensity estimated using 10-hold cross validation was compared with the actual measured values, which resulted in a root mean square error of 9.87%. This estimation equation for BLB damage intensity was input into the satellite data, and the spatial distribution of the BLB damage intensity was visualized. A map of the BLB damage intensity created after the visualization is shown in Figure 11.

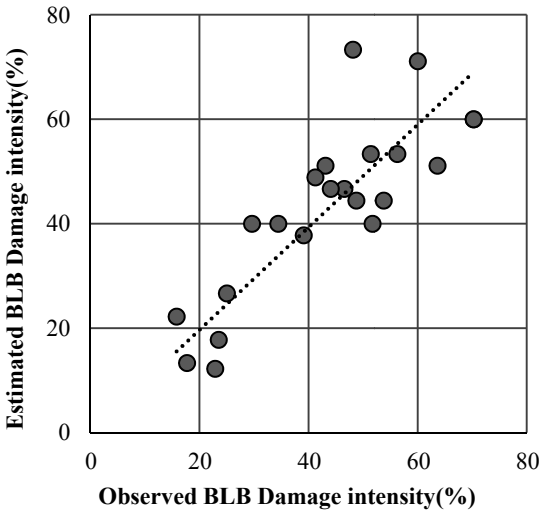


Figure 11. Comparison between estimated values using 10-hold cross validation and actual measurements

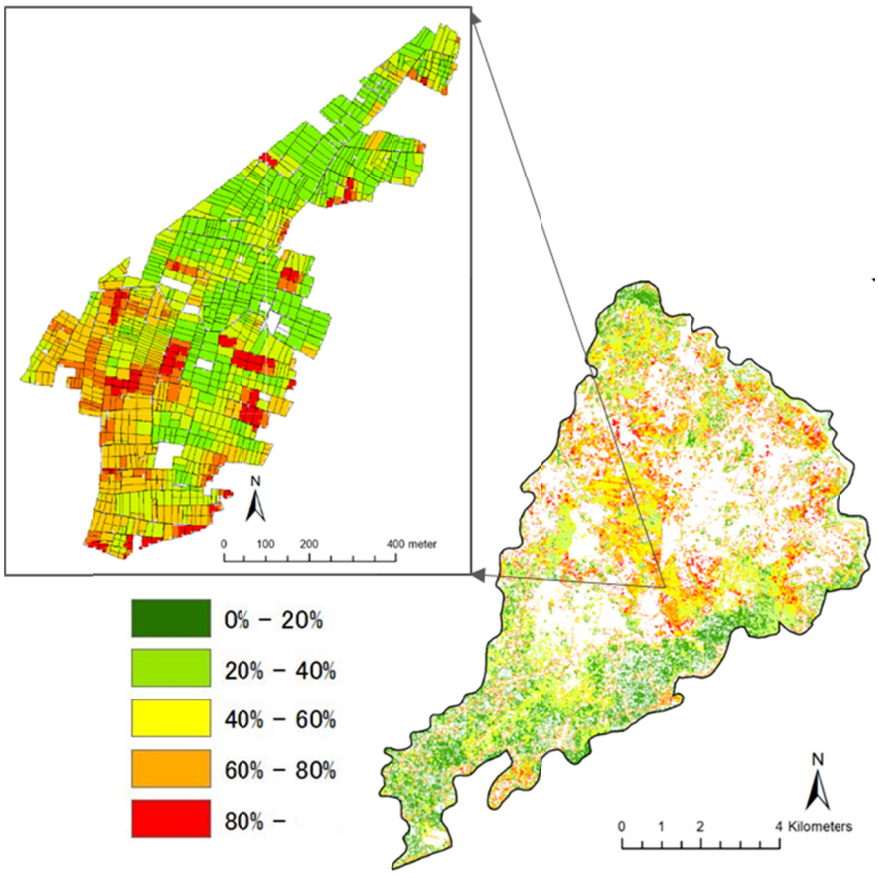


Figure 12. Map of bacterial leaf blight (BLB) damage intensity

## 4. Conclusions

In this study, we attempted to create a new method for assessing damage to crops caused by pests and diseases using remote sensing data. This will enable a more efficient and accurate damage evaluation system for payment of indemnity in the agricultural insurance system of Indonesia, which was formally operationalized in 2016. In this study, the relationships between the BLB damage degree evaluated by pest observers using the current visual inspection method and the reflectance of each observation band of RapidEye, NDVI, GNDVI, and RGI derived

from the satellite data captured on July 17, 2017 were studied. Considering the symptoms of BLB infection, that is, decomposition of chlorophyll in leaves, loss of rice plant vitality, and changes in the green color of the leaves, it was assumed that a positive relation of the infection could be observed with the red edge band and RGI. A positive relationship was confirmed between the BLB damage intensity and the reflectance of the wavelength in the visible range, which is closely related to the color of the leaf. A particularly strong and positive correlation was confirmed between the red band and BLB damage intensity. With the use of reflectance at the red edge, the BLB damage intensity can be evaluated based on pixels and paddy parcels.

Moreover, to check the exact time of the onset of BLB symptoms on the rice plants and the earliest time before harvesting when the relation between BLB damage intensity and satellite data can be confirmed, a time series analysis was conducted using Sentinel-2 data acquired during different periods: heading and flowering, ripening and maturity, and harvesting. The evaluation of the reflectance of visible bands and red edge suggests that the BLB symptoms did not appear or were at an early stage on June 14, 2017 (the heading and flowering period). Following the changes in plant growth towards the harvesting stage, the correlation between the reflectance of the visible range and the BLB damage intensity increased. In contrast, no correlation was found between the BLB damage intensity and NIR (related to biomass volume) until the harvesting season. One of the reasons for this lack of correlation was the onset of BLB infection after the tillering stage in 2017.

Reviewing the results, it is clear that the BLB infection symptoms can be detected and evaluated approximately one or one and a half months in advance before the harvesting period, although it also depends on the wavelength range used. Through this study, we demonstrated that BLB damage intensity can be calculated from satellite data, whereas the current practice involves visual inspection by a pest observer. This means that the satellite sensor could play a role similar to that of the human eye. In addition, remote sensing data can enable us to comprehensively evaluate all paddy plots across a wide area of investigation, whereas the current method covers only three paddy plots at a time in the investigation area.

**Acknowledgements**

Mr. Dede Ruswana, Mr. Yogi Tojiri Septiadi, Mr. Hasam Supriatna, Mr. Gagan Gandana Wibawa, Mr. Adam Daniel, Mr. Denny Magria and Mr. Taufik Rahmat from Provincial Office of Food Crops and Horticulture of West Java Province, Indonesia contributed to this research and field investigation in the project study site.

Funding for this research was provided by Japan Science and Technology Agency (JST) and Japan International Cooperation Agency (JICA). Grant Number: JPMJSA1604.

**References**

Chwen-Ming, Y. (2010). Assessment of the severity of bacterial leaf blight in rice using canopy hyperspectral reflectance. *Precision Agric, 11*, 61-81. https://doi.org/10.1007/s11119-009-9122-4

Clevers, J. G. P. W., & Lammert, K. (2012). Using Hyperspectral Remote Sensing Data for Retrieving Canopy Chlorophyll and Nitrogen Content. *IEEE Journal of Selected Topics in Applied Earth Observations and Remote Sensing, 5*(2), 574-583. https://doi.org/10.1109/JSTARS.2011.2176468

Cleversa, J. G. P. W., & Gitelsonb, A. A. (2013). Remote estimation of crop and grass chlorophyll and nitrogen content using red-edge bands on Sentinel-2 and -3. *International Journal of Applied Earth Observation and Geoinformation, 23*, 344-351. https://doi.org/10.1016/j.jag.2012.10.008

Das, P. K., Laxman, B., Kameswara Rao, S. V. C., Seshasai, M. V. R., & Dadhwal, V. K. (2015). Monitoring of bacterial leaf blight in rice using ground-based hyperspectral and LISS IV satellite data in Kurnool, Andhra Pradesh, India. *International Journal of Pest Management, 61*(4), 359-368. https://doi.org/10.1080/09670874.2015.1072652

Encyclopaedia Britannica. (2020), *Rice bacterial blight*. Encyclopaedia Britannica, Inc. Retrieved from https://www.britannica.com/science/rice-bacterial-blight

FAO (Food and Agriculture Organization of the United Nations). (2006). *Policy Brief*. FAO, Rome.

FAOSAT, Food and Agriculture Organization of the United Nations. (2018a). Retrieved from http://www.fao.org/faostat/en/#data/OA

FAOSAT, Food and Agriculture Organization of the United Nations. (2018b). Retrieved from http://www.fao.org/faostat/en/#data/QC

Ferran, G., Olivier, T., Mathieu, J., Benjamin, F., Jérôme, L., Vincent, L., … Valérie, F. (2016). *Copernicus Sentinel-2 Calibration and Products Validation Status* (Preprint). https://doi.org/10.20944/preprints201610.0078.v1

IPCC (Intergovernmental Panel on Climate Change). (2014). *Fifth Assessment Report (AR5)*. Retrieved from https://www.ipcc.ch/report/ar5/syr

IPCC (Intergovernmental Panel on Climate Change). (2019). Food Security. *An IPCC Special Report on climate change, desertification, land degradation, sustainable land management, food security, and greenhouse gas fluxes in terrestrial ecosystems* (Chapter 5).

Julian, D. C., Francisco, C., Diego, M., Eliel, P., Juan, P. R., Edgar, S. C., … Andres, J.-B. (2020). A novel NIR-image segmentation method for the precise estimation of above-ground biomass in rice crops. *PLoS ONE, 15*(10), e0239591. https://doi.org/10.1371/journal.pone.0239591

Krishnan, N., Gandhi, K., Mohammed, F. P., Muthuraj, R., Kuppusamy, P., & Thiruvengadam, R. (2009). Management of Bacterial Leaf Blight Disease in Rice with Endophytic Bacteria. *World Applied Sciences Journal, 28*(12), 2229-2241. https://doi.org/10.5829/idosi.wasj.2013.28.12

PLANET.COM. (2016). Product Radiometry and Radiometric Accuracy. *RapidEye™ Imagery Product Specifications*. PLANET.COM.

Taifeng, D., Jiangui, L., Budong, Q., Liming, H., Jane, L., Rong, W., … Jiali, S. (2020). Estimating crop biomass using leaf area index derived from Landsat 8 and Sentinel-2 data. *Journal of Photogrammetry and Remote Sensing, 168*, 236-250. https://doi.org/10.1016/j.isprsjprs.2020.08.003

Zhou, X., Zheng, H. B., Xu, X. Q., He, J. Y., Ge, X. K., Yao, X., …Tian, Y. C. (2017). Predicting grain yield in rice using multi-temporal vegetation indices from UAV-based multispectral and digital imagery. *ISPRS Journal of Photogrammetry and Remote Sensing, 130*, 246-255. https://doi.org/10.1016/j.isprsjprs.2017.05.003